Stepwise Behavior of Free Recovery Processes after Diffused Vacuum Arc Extinction

Zhenxing Wang, Yingsan Geng and **Zhiyuan Liu**
State Key Laboratory of Electrical Insulation and Power Equipment
Xi'an Jiaotong University
Xi'an, 710049, China

ABSTRACT

The objective of this paper is to gain insight into free recovery processes in vacuum interrupters after diffused vacuum arcs extinction. A sub-microsecond voltage impulse, which peaked at 90 kV with a rising time of 150 ns) (rate of rise 480 kV/μs), were electronically controlled to apply upon a switching gap of a vacuum interrupter at a predetermined interval after a power frequency current zero. Based on the breakdown voltages at different intervals after arc extinction, we can obtain the free recovery behavior of the vacuum interrupter. The contact materials under study included Cu, CuCr25 and CuCr50. The contacts were butt-type, and the contact diameters were 12 and 25 mm, respectively. The arc current peaked at 2.1 kA with a frequency of 50 Hz and the arcing time was ~9 ms. The results show the free recovery behavior stepped from ~28 kV to ~70 kV at ~4 μs after arc extinction for the three kinds of contact materials with the two contact diameters given. By calculation of the dissipation of metal vapor density and ion density, we conclude that the decay of ions, rather than metal vapor, may be the main reason for the stepwise behavior of the free recovery process after diffused vacuum arcs extinction.

Index Terms — **Vacuum interrupters, vacuum breakdown, free recovery process, dielectric recovery, diffused vacuum arc**

1 INTRODUCTION

DIELECTRIC recovery behavior after current zero is especially important for a vacuum circuit breaker (VCB) because it ultimately determines the interruption capacity of the VCB [1, 2]. As the current in a vacuum interrupter approaches sinusoidal zero, cathode spots, which are the sources of emission, gradually turn off until the final cathode spot ceases to function. However, the interruption process does not come to an end at that time because many particles produced in the arcing period remain in the switching gap including metal vapor [1, 3], ions [4], and droplets [5]. Therefore, the ability of the switching gap to withstand high voltage is finally reached until the residual particles dissipate from the switching gap. Moreover, a transient recovery voltage (TRV) is immediately applied upon the switching gap after current zero. If the dielectric strength of the gap cannot withstand the rapidly rising voltage, a re-ignition may occur. This physical process of dielectric recovery after current zero develops very quickly, and the time scales for the residual particles to disperse are different. The decay of metal vapor density may last for several milliseconds [5, 6], while ions may take only a few microseconds to dissipate from the gap [5, 7]. The density of these residuals depends on the contact material, the arcing time, the amplitude of arc current, and the magnetic field of contacts.

Although researchers seem to be more concerned with dielectric recovery after high current interruption, the experimental results from low current interruption may reveal some fundamental information about interruption processes because the condition after the low current interruption can be relatively simple. For example, when a stationary anode spot forms, the contact surfaces melt where they are attached to the arc roots and continue to evaporate metal vapor after current zero. In addition, the contact surfaces are roughened due to the effect of high energy input from the vacuum arcs [8]. In fact, there are a variety of ways to interpret the failure of high current interruption. However, the experiments using low current can be carried out under specified conditions, reducing the complexity of the process. So, the low current experiments help us to discover the nature of the dielectric recovery processes. It is fundamental to understand the recovery processes after vacuum arc extinction under a "free" condition (i.e., without the influence of a high TRV). Moreover, the knowledge of free recovery behaviors after diffuse vacuum arcs extinction forms a basis for further understanding the dielectric recovery process of a vacuum interrupter under TRV.

The objective of this paper is to gain insight into free recovery processes in vacuum interrupters after diffuse vacuum arcs extinction. We adopt a sub-microsecond voltage impulse that peaks at 90 kV with a rising time of 150 ns (rate of rise 480 kV/μs). The voltage impulses can be electronically

Manuscript received on 2 March 2011, in final form 9 August 2011.

controlled to apply upon a switching gap at a predetermined interval of time after a power frequency current zero. The contact materials in the tested vacuum interrupters include copper (Cu), copper-chromium using 25% weight chromium (CuCr25), and copper-chromium using 50% weight chromium (CuCr50) contact materials. The contact diameters are 12 and 25 mm, respectively. The dielectric recovery behaviors are measured within 15 μs after current zero with a peak arc current of 2.1 kA. At the end, the paper discusses the effect of residual particles on the free recovery processes after interrupting a diffuse vacuum arc.

2 EXPERIMENT

2.1 TEST SPECIMEN

Figure 1 shows the structure of a tested vacuum interrupter. The diameters of the butt-type contacts were 12 and 25 mm, respectively. The thickness of the contact plate was 4mm. Three kinds of contact materials were used in the experiments: oxygen-free high-conductivity Cu (OFHC), CuCr25 and CuCr50. All of the vacuum interrupters were conditioned by low currents before the experiments.

In order to confirm that the vacuum arcs remained in a diffuse mode, we had to observe the arc modes before measuring the recovery processes. Thus, we specifically used several vacuum interrupters that had an observation window (40 mm × 40 mm) on the stainless-steel shield and the insulation envelopes of the vacuum interrupters were made of glass.

After confirming the vacuum arc mode, we used commercial vacuum interrupters with the same structure as shown in Figure 1 except that the shield did not have a window for the recovery experiments.

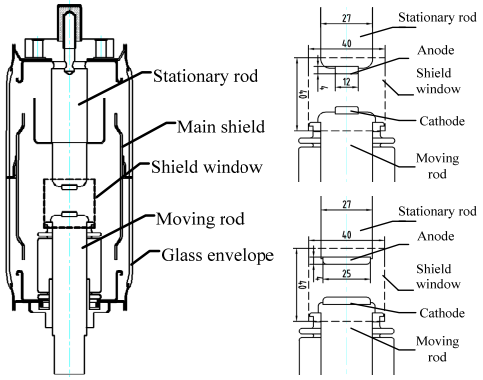

Figure 1. Sketch of a tested vacuum interrupter. The upper electrode was fixed in the position; the lower one was able to move. Contact diameters were 12mm and 25mm, respectively.

2.2 EXPERIMENTAL SETUP

Experiments were conducted using the apparatus shown schematically in Figure 2. The arc current was provided by an L-C discharging circuit. A drawn arc was initiated between a pair of butt contacts in a tested vacuum interrupter. In the initial condition, the main switch (SW1) was opened, and the auxiliary switch (SW2) was closed. A test switch (TSW), in which a tested vacuum interrupter was assembled, was kept closed. In addition, SW1, SW2, and TSW were driven by permanent magnetic actuators to efficiently control close/open time accuracy. Before the experiments, the capacitor banks were charged to an appropriate voltage that controlled a discharging arc current. First, SW1 was closed, which initiated a power frequency current of 50 Hz passing through the reactors L. After a predetermined interval to control the arcing time, TSW and SW2 were electronically controlled to open at the same time by the permanent magnetic actuators. In this way, the first half-wave of the initiated discharging current passed through the tested vacuum interrupter and an arc was drawn. The predetermined open time of TSW and SW2 can adjust the arcing time from 1ms to 9 ms. In the following tests, the arcing time was set to 9 ms if the vacuum arc was extinguished at the first current zero point. Then, a negative voltage impulse was applied to a pair of contacts of the tested vacuum interrupter through a current-limiting resistor R (50 Ω) after a predetermined interval ΔT that can be adjusted from 0μs to 15 μs as shown in Figure 3. After repeating the application of the voltage impulses, we can obtain the free recovery behaviors of a tested vacuum interrupter from 0 μs to 15 μs after current zero.

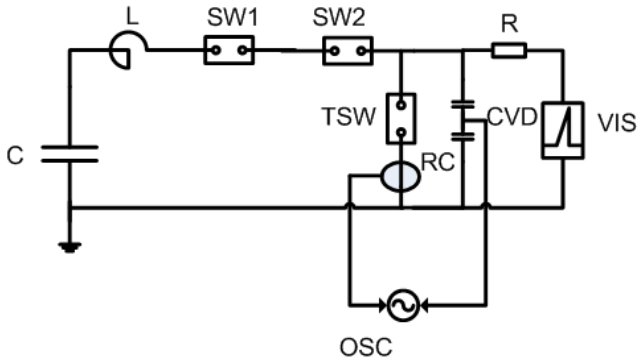

Figure 2. Sketch of experimental circuit. C: Capacitor banks; L: Reactors; SW1: Main switch; SW2: Auxiliary switch; TSW: Test switch with a tested vacuum interrupter involved; R: Resistor (50 Ω); CVD: Capacitive voltage divider (3 pF, 4.2:1); VIS: Voltage impulse source; RC: Rogowski coil; OSC: Oscilloscope.

Figure 4 shows a waveform of a voltage impulse that was generated by a voltage impulse source (VIS) and can be controlled electronically to apply voltage impulses to a vacuum interrupter. The impulse peaked at 90 kV with a rising time of 150ns (rate of rise 480 kV/μs) and measured by a Tektronix high-voltage probe P6015A (1000:1) through a capacitive voltage divider (CVD) (3 pF, 4.2:1). The arc current was measured by a Rogowski coil.

For the permanent magnet operating mechanism, the average opening velocity remained quite stable during the experiments. The opening velocity for the tested vacuum interrupters was 1.2 m/s, and the scatter of the arcing time was controlled below 1 ms. The gap length of the tested vacuum interrupter was measured as ~10 mm when the voltage impulses were applied to the contacts. To ensure the accuracy of gap length at current zero, we used a KTC-100 type linear displacement transducer to measure the displacement of the actuator during the experiments, as shown in Figure 5.

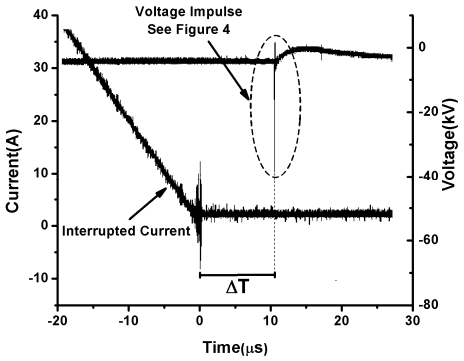

Figure 3. Waveforms around current zero point. A negative voltage impulse was applied to a pair of contacts of a tested vacuum interrupter after a predetermined interval Δ T. The detailed waveform of the impulse is shown in Figure 4.

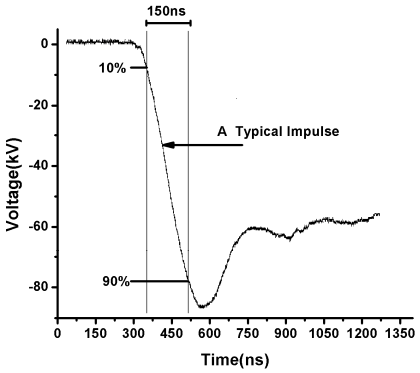

Figure 4. Waveform of a voltage impulse. The impulse peaked at 90 kV with a rising time of 150 ns (rate of rise ~480 kV/μs).

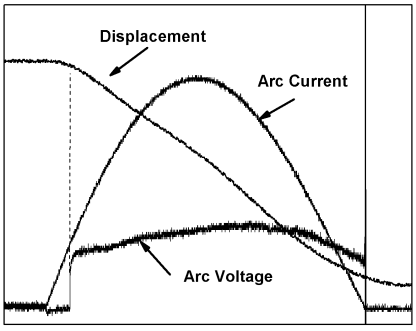

Figure 5. Waveform of arc current, arc voltage, and displacement curve of moving contact.

A high-speed charge-coupled device (CCD) video camera Phantom V10 was used to record the evolution of the vacuum arc modes in the experiments. The recording velocity was set to 4000 frames per second. The camera aperture was fixed at 4, and the exposure time was set at 2 μs.

3 RESULTS

3.1 THE OBSERVATION OF VACUUM ARCS

As shown in Figure 6 the arc voltages for the three kinds of contact materials remained in the range of 10 to 35 V and appeared smooth during the arcing period. Figure 7 through Figure 12 show an observation of vacuum arcs of Cu, CuCr25, and CuCr50 contact materials until 2.1 kA arc current (peak value) extinction. The upper contacts were anodes, and the lower contacts were cathodes. Figure 7 through Figure 8 show the cases where contact diameter was 12 mm and the contact materials were Cu, CuCr25, and CuCr50, respectively. Figure 10 through Figure 12 show the cases where contact diameter was 25 mm and the contact materials were Cu, CuCr25, and CuCr50, respectively. As shown in Figure 7 toFigure **12**, the vacuum arcs for the three materials remained in a diffuse arc mode during the arcing period. Moreover, the anode in the experiments acted as a passive collector of electrons which were emitted from cathode spots without anode spots or foot point formed on the contacts.

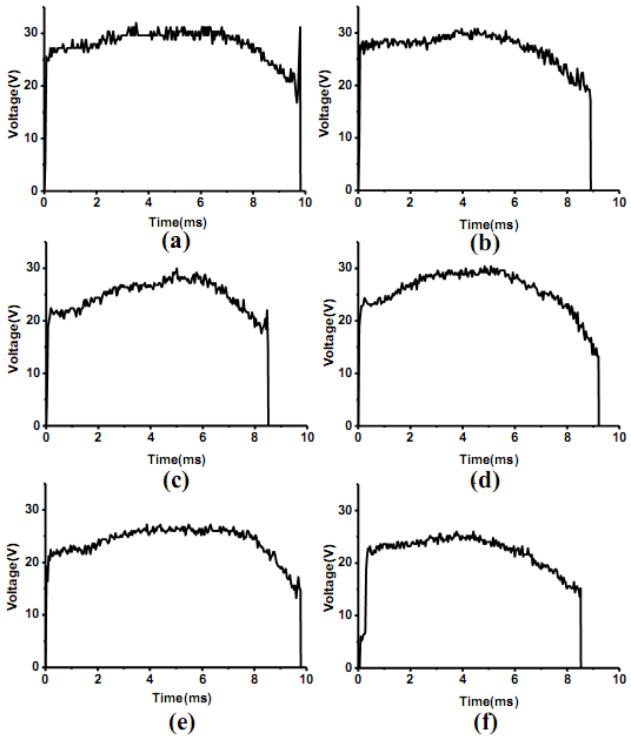

Figure 6. Arc voltage. Peak current: 2.1 kA. (a): Cu, Φ=12 mm; (b): Cu, Φ =25 mm; (c): CuCr25, Φ=12 mm; (d): CuCr25, Φ=25 mm; (e): CuCr50, Φ =12 mm; (f): CuCr50, Φ=25 mm;

3.2 MEASUREMENT OF FREE RECOVERY BEHAVIORS AFTER EXTINCTION

Figure 13 through Figure 15 show free recovery behaviors of Cu, CuCr25, and CuCr50 contact materials after 2.1 kA arc current (peak value) extinction , which was below a threshold current of appearing high current anode phenomena. The contact diameters were 12 and 25 mm, respectively. After repeating the application of the voltage impulses, we obtained the free recovery behaviors of the tested vacuum interrupters. In Figure 13 through Figure 15, the crosses represent that the gap could not withstand the voltage impulse at that instant, and the circles indicate that no breakdown occurred.

As Figure 13 through Figure 15 show, the breakdown voltage did not increase continuously after current zero. However, the figures do show a stepwise behavior in the free recovery process and the voltage stepped from ~28 to ~70 kV at ~4 μs after current zero. The stepwise free recovery behavior dominated all the investigated contact materials and contact diameters. The measured data can be divided into three zones: a low voltage zone, a high voltage zone, and a transition zone.

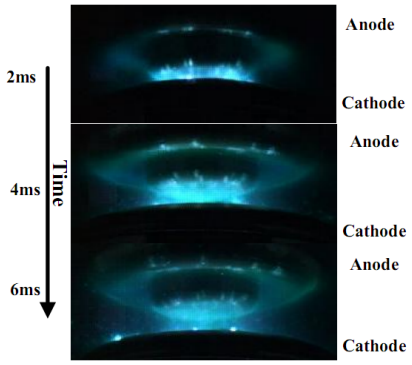

Figure 7. Vacuum arc images of Cu contacts. Peak current: 2.1 kA. Contact diameter: 12 mm. The time indicates the amount of time from contact separation.

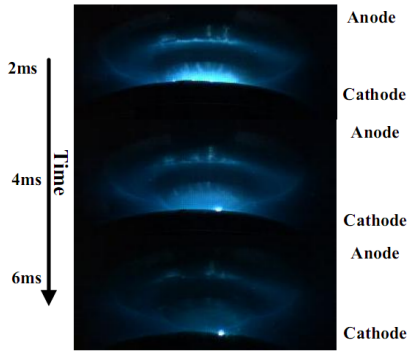

Figure 8. Vacuum arc images of CuCr25 contacts. Peak current: 2.1 kA. Contact diameter: 12 mm. The time indicates the amount of time from contact separation.

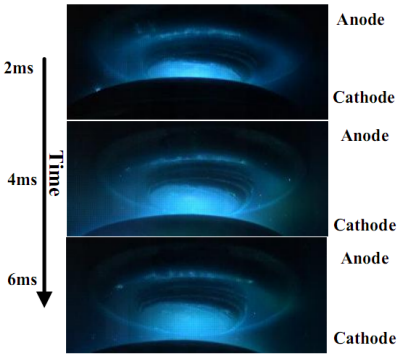

Figure 9. Vacuum arc images of CuCr50 contacts. Peak current: 2.1 kA. Contact diameter: 12 mm. The time indicates the amount of time from contact separation.

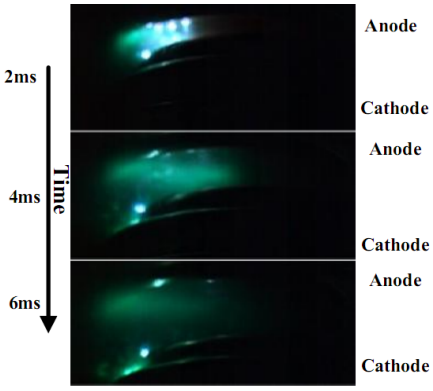

Figure 10. Vacuum arc images of Cu contacts. Peak current: 2.1 kA. Contact diameter: 25 mm. The time indicates the amount of time from contact separation.

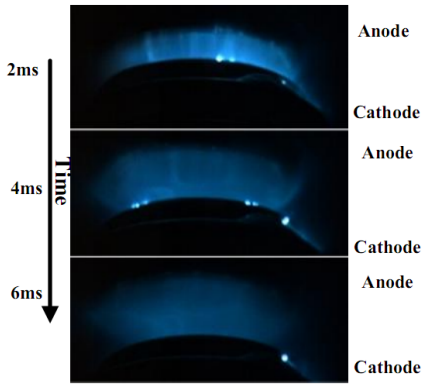

Figure 11. Vacuum arc images of CuCr25 contacts. Peak current: 2.1 kA. Contact diameter: 25 mm. The time indicates the amount of time from contact separation.

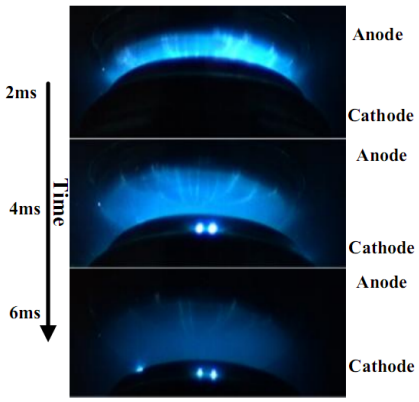

Figure 12. Vacuum arc images of CuCr50 contacts. Peak current: 2.1 kA. Contact diameter: 25 mm. The time indicates the amount of time from contact separation.

In the low voltage zone, which began from 0μs to ~4 μs after current zero, the breakdown voltage fluctuated between 15 kV and 45 kV, and the mean breakdown voltage for the three contact materials was 28 kV (contact diameter:12 and 25 mm).

In the transition zone, which began from 3 to 6 μs after arc extinction and the medium value for the stepping was ~4 μs, the breakdown voltage rose from ~28 to ~70 kV. The width variation of the transition zone was from 1 to 3 μs.

In the high voltage zone, which began from ~4 to ~15 μs after current zero, the mean breakdown voltages for the three kinds of materials leveled off at ~70 kV. Also, we observed that the voltage pulses impressed across the contact gaps did not lead to a breakdown every time. Moreover, the contact diameters (12 and 25 mm) have little influence on the final breakdown voltage for the same contact material.

4 DISCUSSION

As shown in Figure 13 through Figure 15, there is a stepwise jump of the breakdown voltage in the free recovery processes. The voltage stepped from ~28 to ~70 kV at ~4 μs after current zero indicating a fast recovery process following

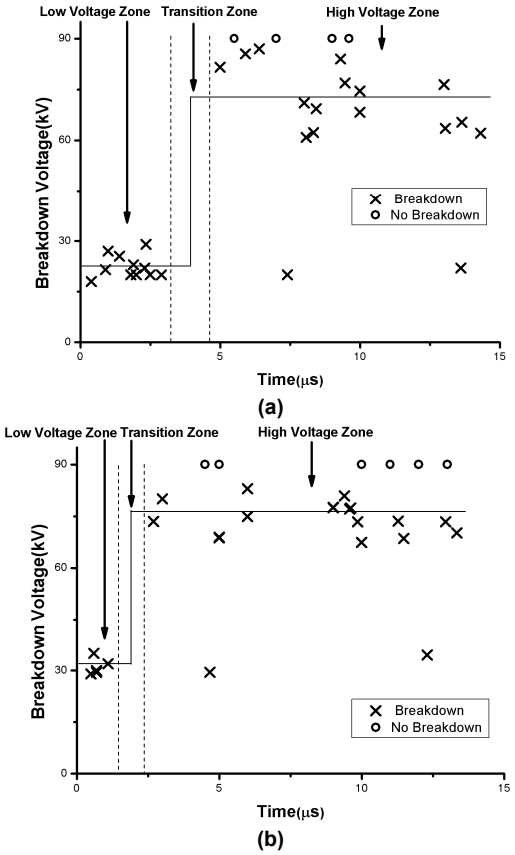

Figure 13. Dielectric recovery behaviors of Cu contacts. Contact diameter: (a) Φ =12 mm; (b) Φ=25 mm. Cross: breakdown voltage; Circle: no breakdown occurred.

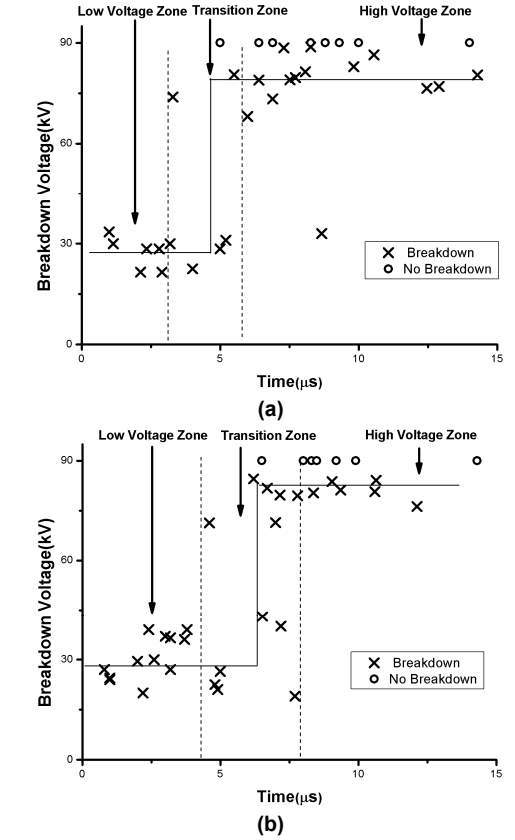

Figure 14. Dielectric recovery behaviors of CuCr25 contacts. Contact diameter: (a) Φ=12 mm; (b) Φ=25 mm. Cross: breakdown voltage; Circle: no breakdown occurred.

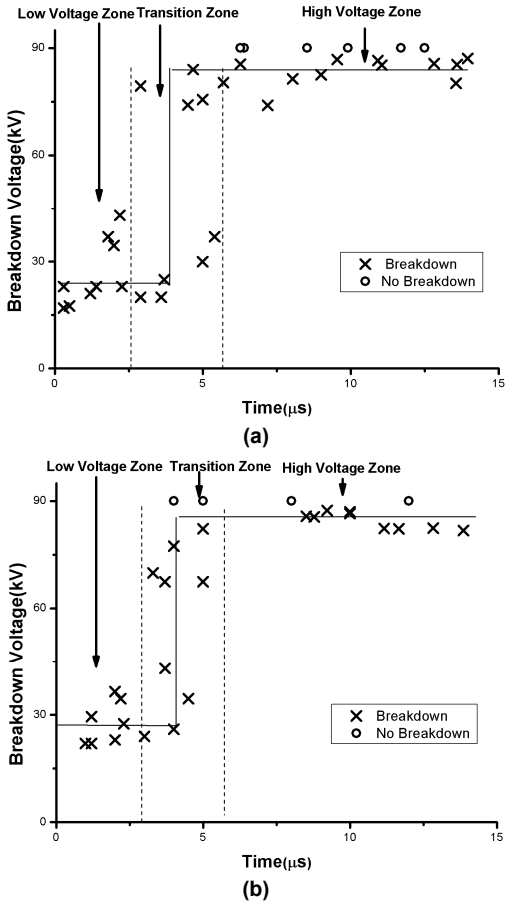

Figure 15 . Dielectric recovery behaviors of CuCr50 contacts. Contact diameter: (a) Φ=12 mm; (b) Φ=25 mm. Cross: breakdown voltage; Circle: no breakdown occurred.

a low current extinction. The stepwise free recovery processes may be caused by the decay of residual particles such as metal vapor, ions, and droplets. The particles that are produced during the arcing time remain in the gap after current extinction and decay over time. In this section, we will discuss the effect of metal vapor and ions during the recovery process and interpret the stepwise behavior in the experiments.

4.1 THE EFFECT OF METAL VAPOR

First, we consider the effect of metal vapor in a free recovery process. It is difficult to find an accurate model to describe the metal vapor recovery process because of its complexity. However, the model of Rich and Farrall [9] provides us with a quantitative way to calculate metal vapor density after current extinctions.

We adopt the formula of Lins [10] to calculate the initial density of the metal vapor n after current extinction:

$$n(t) = \frac{S_m}{\omega^2 + \beta^2}(\beta \sin \omega t - \omega \cos \omega t + \omega e^{-\beta t}) \quad (1)$$

where S_m is the rate at which the metal atom is evaporated from contact surfaces, β represents the particle loss per second at the bounding surfaces of the gap volumes, and ω is the angular frequency of the current. Moreover,

$$S_m = \frac{KI_m E}{mV} \quad (2)$$

where E is the erosion rate of the contact materials, I_m is the peak value of currents, m is the mass of a metal atom, and K is a parameter to adjust metal vapor generation rates. $V = \pi R^2 L$ represents the gap volume where R is the radius of the contact and L is the gap length. In addition, if we assume that the condensation coefficients C_i for the contact surfaces are equal to 1, the particle loss rate can be rewritten as:

$$\beta = \frac{\bar{v}\sum A_i C_i}{4V} = \sqrt{\frac{8kT}{\pi m}} \frac{2\pi RL + \pi R^2}{4\pi R^2 L} \tag{3}$$

where v is mean thermal velocity, A_i is the surface area of the ith surface, C_i is the condensation coefficient of ith surface, m is the mass of a metal atom, k is Boltzmann's constant, and T is the temperature of metal vapor. We used 2000 K as the metal vapor temperature [11-13]. We employed 115 μg/C [14], 33.2 μg/C, and 31 μg/C [15] as the erosion rates for Cu, CuCr25 and CuCr50 contact materials, respectively. In addition, we set K at 8% as Lins did [10].

The expression for the metal vapor density at the center of the gap volume at time t after current extinction can be described by:

$$n(0, \frac{L}{2}, t) = n_0[1 - e^{-\frac{1}{\alpha^2}}] erf[\frac{1}{2}(\frac{L}{R})(\frac{1}{\alpha})] \tag{4}$$

where $\alpha = \frac{t}{R}\sqrt{\frac{2kT}{m}}$ and $erf(x) = \frac{2}{\sqrt{\pi}}\int_0^x e^{-t^2} dt$ represents an error function. So, the decay of the metal vapor density for those contacts with a contact diameter of 12mm in our experiments is shown in Figure 16 and the decay for those contacts with a diameter of 25 mm is shown in Figure 17.

As shown in Figure 16 and Figure **17**, the initial densities of the metal vapor for the three contact materials are of the same order of 10^{18}/m^3 and decay exponentially over the recovery time. Furthermore, the calculated results are similar to the experimental results obtained by Lins [6], Gellert et al [12], and Takahashi et al [16]. Rich and Farrall [9] concluded that the decay of metal vapor dominates the recovery process after a diffuse vacuum arc extinction and that the recovery process will end when the metal vapor density drops below the level where the electron's mean free path in the vapor is similar to the gap length. Frind et al [17] confirmed this conclusion by investigating the recovery process after interrupting a high current that was above the threshold to form an anode spot.

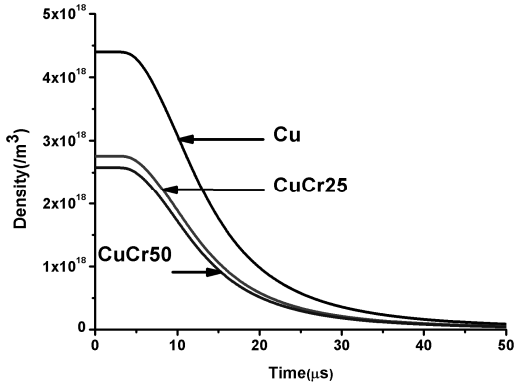

Figure 16. Decay over time of the metal vapor density for contacts with a diameter of 12 mm.

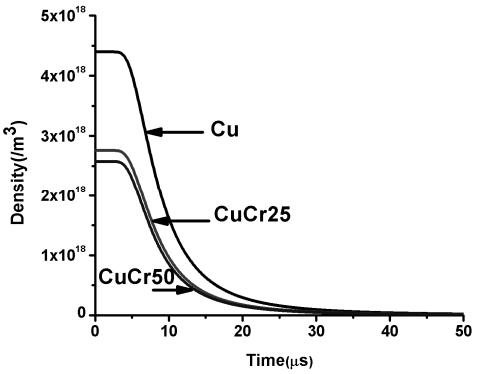

Figure 17. Decay over time of the metal vapor density for contacts with a diameter of 25 mm.

However, we may not attribute the stepwise free recovery process in our experiments to the decay of the metal vapor. It is shown in Figure 16 and Figure 17 that the fast decay of metal vapor density ranges on the order of ~10 μs rather than ~4 μs, as shown in Figure 13-Figure **15**. So, the metal vapor dissipation cannot explain the stepwise behaviors in the experiments in the sense of time scale. Schade and Dullni [2] proposed a critical value of n×d=3×10^{19}/m^2 to determine an instant breakdown. If the product of metal vapor density and contact gap is below the critical value, breakdown may be attributed to a type of delayed breakdown. In our case, the maximum value of n×d is 5×10^{16}/m^2, which is three order lower than the critical value. Since the arc current in the tests was so low and the arc mode was in a diffuse mode, metal vapor density decayed while the arc was still burning. Thus, only a small quantity of metal vapor remained after arc extinction, in contrast to a high current interruption. Therefore, the reason for the free stepwise dielectric recovery behavior after current zero cannot be due to metal vapor alone.

4.2 THE EFFECT OF IONS

Residual plasma which is composed of ions and electrons also has influence on dielectric recovery processes. There are many researchers [4, 18, 19] who focused on sheath development when a TRV is applied upon the residual plasma resulting in a post-arc current after current zero. After current zero, the voltage across the inter-electrode plasma changes its polarity. Under the influence of the TRV the electrons quickly reverse their moving direction toward the post-arc anode, and the heavier positive ions first remain there. Thus, a sheath forms in front of the post-arc cathode and develops toward the post-arc anode associated with a post-arc current. This sheath takes the whole TRV. When the sheath is too small，breakdown occurs.

In this paper, a simpler situation is considered - a free dielectric recovery process, which means there is no TRV applied in a dielectric recovery process of a vacuum interrupter. In such a situation, the post-arc current is not notable. However, in this simpler situation, one is easier to focus on a "free" dissipation process of the inter-electrode particles. Based on an understanding of the free dielectric recovery process, one is possible to get further insight of a dielectric recovery process in a vacuum interrupter under TRV.

In the free recovery process the decay rate of ions is much slower than that of electrons. Although the ions may dissipate from the switching gap in ~1 μs based on the calculation of the Maxwellian velocity distribution [1], some experimental results [4, 18, 20] indicated that the decay time for the ions may be longer than the time calculated by the Maxwellian velocity distribution function. In other words, some ions that have very low velocities may remain after interrupting a vacuum arc, and Dullni et al. called them "slow ions" [3]. However, the Rich-Farrall model is not applicable in the "slow ion" case because the effect of collisions is not considered.

In order to calculate the decay time of the ions, we adopt a Particle in Cell – Monte Carlo Collision (PIC-MCC) method to describe an ion transport after vacuum arc extinction. The method consists of four modules including movement module, collision module, weighting module and electric field calculation module as shown in Figure 18. In the particles movement module, one can obtain the motion of charged particles by solving Newton's equation:

$$\frac{d\vec{v}}{dt} = \frac{q\vec{E}}{m} \tag{5}$$

where v is the velocity of the charged particles, q is the electric charge, m is the mass of the charged particles, and E is the electric field that forces charged particles to move. The collision module is used to model collisions between particles and background neutrals by the Monte Carlo method based on atomic cross-sections. The weighting module obtains the density of the charged particles and distributes them to the cell grids. The electric field module calculates the electric field at grids by solving Poisson's equation:

$$\nabla^2\varphi = -\frac{e}{\varepsilon_0}(n_i - n_e) \tag{6}$$

where φ is the electric potential of the field, ε_0 is the vacuum permittivity, e is electron charge, n_i is ion density, and n_e is electron density. Furthermore, the electric field force is provided to the movement module, which continues to simulate the motion of the charged particles. A review of the PIC-MCC method can be found in [21].

With the aid of PIC-MCC method, one can calculate the decay rate of Cu ions in free recovery processes considering the collisions between the charged particles and background neutrals. A 2D cylindrical model is developed with a gap length of 10 mm between the contacts. The contact diameters are 12 and 25 mm, respectively. The initial plasma density is $10^{17}/m^3$[7] which was measured by Lins after artificial interruption of a sinusoidal current of 200 A. The background neutral density is $10^{18}/m^3$ in accord with section 4.1. We assume a Maxwellian velocity distribution for the ions and electrons at temperature 0.2 and 1 eV [22-25] at the start of free recovery. We consider the influence of ion-neutral and electron-neutral collisions. The cross-section curve for Cu atoms can be found in [26]. There is no secondary emission from the contact surfaces considered during the simulation processes, and the charged particles are absorbed by the boundaries when the particles achieve the boundaries of the model. The grid spacing is equal to one Debye length and the time step is equal to a tenth of plasma oscillation period.

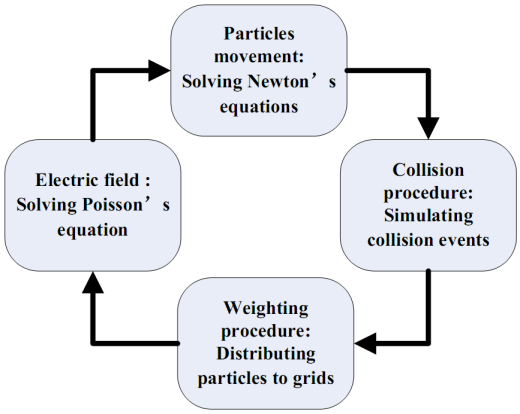

Figure 18. Computing sequence for PIC-MCC method.

As shown in Figure 19, the ion density was $10^{17}/m^3$ at current zero and dropped to $10^{14}/m^3$ in ~4 μs, taking into account the collision effect. However, if the ions leave the gap freely without the collisions, the ion density dropped from $10^{17}/m^3$ to $10^{14}/m^3$ in ~0.5 μs. The decay time for the ions without the collisions is much faster than it is with the collisions. The decay rates calculated in our model are similar to the results measured by Lins [7]. Moreover, the ion density falls by three orders of magnitude in ~4 μs.

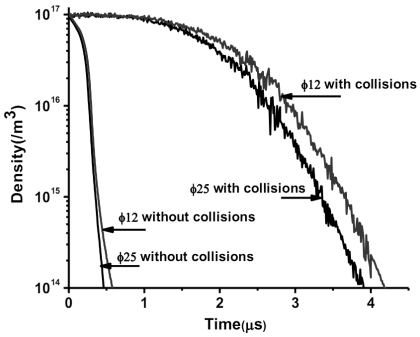

Figure 19. Decay over time of the ion density for contacts with a diameter of 12/25 mm. The initial ion density is assumed to be a Maxwellian velocity distribution. Contact material: Cu; Ion temperature: 0.2 eV; Electron temperature: 1 eV.

The decay of the ions may have a strong impact on the free recovery behaviors after current zero. Compared to the decay time scale for the metal vapor ~10 μs, the decay time scale ~4μs for the ions is much closer to the time point of the stepwise behavior when the breakdown voltage jumped. The ion density falls by three orders of magnitude while the metal vapor density remains almost constant. Thus, the explanation for the stepwise behavior of the free recovery is more likely to be related to the influence of the ions rather than that of the metal vapor. Nevertheless, metal vapor, which serves as background neutrals, still be necessary for breakdown to occur. According to the calculation by Wang et al [27], the residual charge after extinction has a significant influence on the distribution of the electric field in vacuum interrupters. They pointed out that if the residual charge reaches a certain value, the electric field intensity on the surface of the contacts and shields may rise steeply and this has a significant influence the breakdown effect of the vacuum interrupters.

On the basis of the above analysis, we intend to attribute the stepwise breakdown behavior in a free dielectric recovery process after interrupting a diffuse vacuum arc to an ion-assisted breakdown. The possibility of a breakdown drops with the decay of the ion density, and the voltage impulse cannot initiate a breakdown if the ion density drops to a certain level. Moreover, the metal vapor which plays an effective role in the collision processes also has an influence on the decay of ions.

CONCLUSIONS

We observed the free recovery behaviors of Cu, CuCr25, and CuCr50 contact materials after diffuse vacuum arcs extinction by using a voltage impulse that peaks at 90 kV with a rising time of 150 ns (rate of rise 480 kV/μs). The diameters of the contacts were 12 and 25 mm, respectively. The arc current peaks at 2.1 kA with a frequency of 50 Hz, and the arcing time is about 9 ms. The gap length was about 10 mm when the voltage impulses were applied onto the contacts. In addition, we observed the vacuum arc for the three kinds of materials in order to confirm that the arcs remained in a diffuse mode during the arcing period. The results show that the free recovery behaviors stepped from ~28 to ~70 kV at ~4 μs after arc extinction for the three kinds of contact materials with these two contact diameters. On the basis of calculation results of dissipation of metal vapor and ion density, we conclude that the decay of ions, rather than metal vapor, plays an important role in the free recovery process after interrupting a diffuse vacuum arc. Nevertheless, metal vapor, which serves as background neutrals, still takes an effective role for breakdown to occur.

ACKNOWLEDGMENT

Our sincere acknowledgment goes to the technical support of Dr. Xiaoshe Zhai of Xi'an Jiaotong University. We also want to thank graduate students Peng Yan, Guowei Kong, Sheng Zhang, Bing Dong, and Chenbo Hu for their contributions in the experimental work. We would like to thank Baoguang company, Shaanxi province, China for providing the vacuum interrupters. This work was supported by the National Natural Science Foundation of China under Project No.50777050 and the Fundamental Research Funds for the Central Universities.

REFERENCES

[1] G. A. Farrall, "Recovery of Dielectric Strength after Current Interruption in Vacuum", IEEE Trans. Plasma Sci., Vol. 6, No. 4, pp.360-369, 1978.

[2] E. Schade, and E. Dullni, "Recovery of breakdown strength of a vacuum interrupter after extinction of high currents", IEEE Trans. Dielectr. Electr. Insul., Vol. 9, No. 2, pp.207-215, 2002.

[3] E. Dullni, E. Schade, and B. Gellert, "Dielectric Recovery of Vacuum Arcs after Strong Anode Spot Activity", IEEE Trans. Plasma Sci., Vol. 15, No. 5, pp.538-544, 1987.

[4] S. Yanabu, M. Homma, E. Kaneko, and T. Tamagawa, "Post Arc Current of Vacuum Interrupters", IEEE Trans. Power App. Syst., Vol. 104, No. 1, pp.166-172, 1985.

[5] E. Dullni, and E. Schade, "Investigation of High-Current Interruption of Vacuum Circuit-Breakers", IEEE Trans. Electr. Insul., Vol. 28, No. 4, pp.607-620, 1993.

[6] G. Lins, "Measurement of the Neutral Copper Vapor Density around Current Zero of a 500-a Vacuum-Arc Using Laser-Induced Fluorescence", IEEE Trans. Plasma Sci., Vol. 13, No. 6, pp.577-581, 1985.

[7] G. Lins, "Influence of Electrode Separation on Ion Density in the Vacuum-Arc", IEEE Trans. Plasma Sci., Vol. 19, No. 5, pp.718-724, 1991.

[8] T. Matsuo, H. Fujimori, S. Yanabu, H. Ichikawa, Y. Matsui, and M. Sakaki, "Insulation recovery characteristics after current interruption by various vacuum interrupter electrodes", IEEE Trans. Dielectr. Electr. Insul., Vol. 13, No. 1, pp.10-17, 2006.

[9] J. A. Rich, and G. A. Farrall, "Vacuum Arc Recovery Phenomena", Proceedings of the IEEE, Vol. 52, No. 11, pp.1293-1301, 1964.

[10] G. Lins, "Evolution of Copper Vapor from the Cathode of a Diffuse Vacuum-Arc", IEEE Trans. Plasma Sci., Vol. 15, No. 5, pp.552-556, 1987.

[11] R. L. Boxman, and S. Goldsmith, "The Interaction between Plasma and Macroparticles in a Multi-Cathode-Spot Vacuum-Arc", J Appl Phys, Vol. 52, No. 1, pp.151-161, 1981.

[12] B. Gellert, E. Schade, and E. Dullni, "Measurement of Particles and Vapor Density after High-Current Vacuum Arcs by Laser Techniques", IEEE Trans. Plasma Sci., Vol. 15, No. 5, pp.545-551, 1987.

[13] G. Lins, "Measurement of the Temperature of Evaporating Macroparticles after Current Zero of Vacuum Arcs", IEEE Trans. Plasma Sci., Vol. 16, No. 4, pp.433-437, 1988.

[14] C. W. Kimblin, "Erosion and Ionization in Cathode Spot Regions of Vacuum Arcs", J. Appl. Phys., Vol. 44, No. 7, pp.3074-3081, 1973.

[15] M. B. Schulman, P. G. Slade, and J. A. Bindas, "Effective Erosion Rates for Selected Contact Materials in Low-Voltage Contactors", IEEE Trans Compon. Pack. A, Vol. 18, No. 2, pp.329-333, 1995.

[16] S. Takahashi, K. Arai, O. Morimiya, K. Hayashi, and E. Noda, "Laser measurement of copper vapor density after a high-current vacuum arc discharge in an axial magnetic field", IEEE Trans. Plasma Sci., Vol. 33, No. 5, pp.1519-1526, 2005.

[17] G. Frind, J. J. Carroll, and E. J. Tuohy, "Recovery Times of Vacuum Interrupters Which Have Stationary Anode Spots", IEEE Trans. Power App. Syst., Vol. 101, No. 4, pp.775-781, 1982.

[18] G. Duning, and M. Lindmayer, "Plasma density decay of vacuum discharges after current zero", Proc.Xviiith International Symposium on Discharges and Electrical Insulation in Vacuum (ISDEIV), Eindhoven, The Netherlands, pp.447-454, 1998.

[19] E. P. A. van Lanen, M. Popov, L. van der Sluis, and R. P. P. Smeets, "Vacuum circuit breaker current-zero phenomena", IEEE Trans. Plasma Sci., Vol. 33, No. 5, pp.1589-1593, 2005.

[20] R. Gilles, K. D. Weltmann, E. Schade, and M. Claessens, "Determination of the residual charge after current extinction - An integral approach", Proc.Xixth International Symposium on Discharges and Electrical Insulation in Vacuum (ISDEIV), Xi'an, China, pp.481-484, 2000.

[21] C. K. Birdsall, "Particle-in-Cell Charged-Particle Simulations, Plus Monte-Carlo Collisions with Neutral Atoms, Pic-Mcc", IEEE Trans. Plasma Sci., Vol. 19, No. 2, pp.65-85, 1991.

[22] J. Kutzner, and H. C. Miller, "Integrated Ion Flux Emitted from the Cathode Spot Region of a Diffuse Vacuum-Arc", J Phys D Appl Phys, Vol. 25, No. 4, pp.686-693, 1992.

[23] P. Sarrailh, L. Garrigues, G. J. M. Hagelaar, G. Sandolache, S. Rowe, B. Jusselin, and J. P. Boeuf, "Expanding sheath in a bounded plasma in the context of the post-arc phase of a vacuum arc", J. Phys. D Appl. Phys., Vol. 41, 015203 (11 pp.) 2008.

[24] J. Kutzner, and H. C. Miller, "Ion Flux from the Cathode Region of a Vacuum-Arc", IEEE Trans. Plasma Sci., Vol. 17, No. 5, pp.688-694, 1989.

[25] R. L. Boxman, D. M. Sanders, and P. J. Martin, *Handbook of Vacuum Arc Science and Technology: Fundamentals and Applications*, Noyes Publications: New Jersey, pp. 198-199, 1995.

[26] A. N. Tkachev, A. A. Fedenev, and S. I. Yakovlenko, "Townsend coefficient, escape curve, and fraction of runaway electrons in copper vapor", Laser Physics, Vol. 17, No. 6, pp.775-781, 2007.

[27] Z. Wang, and J. Wang, "Distribution of electric field in vacuum interrupter during interrupting", Proc.Xixth International Symposium on Discharges and Electrical Insulation in Vacuum (ISDEIV), Xi'an, China, pp.471-474, 2000.

This paper is based on a presentation given at the 24th International Symposium on Discharges and Electrical Insulation in Vacuum, TU Braunschweig, Germany, in September 2010.

Zhenxing Wang was born on 10 August 1983. He received the B.S. degree in electrical engineering from Xi'an Jiaotong University, Xi'an, China, in 2006. He is currently working toward the Ph.D. degree in electrical engineering in Xi'an Jiaotong University. He research interests include dielectric recovery in vacuum and vacuum circuit breakers.

Yingsan Geng (M'98) was born in Henan Province, China in 1963. He received the B.S., M.S. and Ph.D. degrees in electrical engineering in 1984, 1987 and 1997, respectively, from Xi'an Jiaotong University (XJTU), China. He is currently a Professor with the State Key Laboratory of Electrical Insulation and Power Equipment, Department of Electrical Engineering, XJTU. His research interests include theory and application of low voltage circuit breaker and high voltage vacuum circuit breakers. Dr. Geng is a Director and Professor of the Department of Electrical Apparatus, Xi'an Jiaotong University.

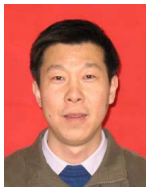

Zhiyuan Liu (M'01) was born in Shenyang, China, in 1971. He received the B.S. and M.S. degrees in electrical engineering from Shenyang University of Technology, Liaoning, China, in 1994 and 1997, respectively. He received the Ph.D. degree in electrical engineering from Xi'an Jiaotong University, Xi'an, China, in 2001. From 2001 to 2002, he was with General Electric Company Research and Development Center (Shanghai), Shanghai, China. Since 2003, he has been working in State key laboratory of electrical insulation and power equipment, department of electrical engineering, Xi'an Jiaotong University, Xi'an, China. Now he is a professor in Xi'an Jiaotong University. He has published more than 50 technical papers. He is primarily involved with research and development of high voltage vacuum circuit breakers. Dr. Liu is a member of current zero club and a member of CIGRE working group WGA3.27 "The impact of the application of vacuum switchgear at transmission voltages".